mathematics

MDPI

Article

Formulation for Multiple Cracks Problem in Thermoelectric-Bonded Materials Using Hypersingular Integral Equations

Muhammad Haziq Iqmal Mohd Nordin [1], Khairum Bin Hamzah [2,3,*], Najiyah Safwa Khashi'ie [2,3], Iskandar Waini [2,3], Nik Mohd Asri Nik Long [4] and Saadatul Fitri [5]

[1] Fakulti Kejuruteraan Pembuatan, Universiti Teknikal Malaysia Melaka, Hang Tuah Jaya, Durian Tunggal 76100, Melaka, Malaysia; m052210026@student.utem.edu.my
[2] Fakulti Teknologi Kejuruteraan Mekanikal dan Pembuatan, Universiti Teknikal Malaysia Melaka, Hang Tuah Jaya, Durian Tunggal 76100, Melaka, Malaysia; najiyah@utem.edu.my (N.S.K.); iskandarwaini@utem.edu.my (I.W.)
[3] Forecasting and Engineering Technology Analysis (FETA) Research Group, Universiti Teknikal Malaysia Melaka, Hang Tuah Jaya, Durian Tunggal 76100, Melaka, Malaysia
[4] Mathematics Department, Faculty of Science, Universiti Putra Malaysia, Serdang 43400, Selangor, Malaysia; nmasri@upm.edu.my
[5] Department of Mathematics, Faculty of Mathematics and Natural Sciences, Brawijaya University, Malang 65145, Indonesia; saadatulfitri@ub.ac.id
* Correspondence: khairum@utem.edu.my

Abstract: New formulations are produced for problems associated with multiple cracks in the upper part of thermoelectric-bonded materials subjected to remote stress using hypersingular integral equations (HSIEs). The modified complex stress potential function method with the continuity conditions of the resultant electric force and displacement electric function, and temperature and resultant heat flux being continuous across the bonded materials' interface, is used to develop these HSIEs. The unknown crack opening displacement function, electric current density, and energy flux load are mapped into the square root singularity function using the curved length coordinate method. The new HSIEs for multiple cracks in the upper part of thermoelectric-bonded materials can be obtained by applying the superposition principle. The appropriate quadrature formulas are then used to find stress intensity factors, with the traction along the crack as the right-hand term with the help of the curved length coordinate method. The general solutions of HSIEs for crack problems in thermoelectric-bonded materials are demonstrated with two substitutions and it is strictly confirmed with rigorous proof that: (i) the general solutions of HSIEs reduce to infinite materials if $G_1 = G_2$, $K_1 = K_2$, and $E_1 = E_2$, and the values of the electric parts are $\alpha_1 = \alpha_2 = 0$ and $\lambda_1 = \lambda_2 = 0$; (ii) the general solutions of HSIEs reduce to half-plane materials if $G_2 = 0$, and the values of $\alpha_1 = \alpha_2 = 0$, $\lambda_1 = \lambda_2 = 0$ and $\kappa_2 = 0$. These substitutions also partially validate the general solution derived from this study.

Keywords: multiple cracks; thermoelectric; bonded materials; hypersingular integral equations; modified complex stress potential

MSC: 74A45; 74G70; 74S70

Citation: Mohd Nordin, M.H.I.; Hamzah, K.B.; Khashi'ie, N.S.; Waini, I.; Nik Long, N.M.A.; Fitri, S. Formulation for Multiple Cracks Problem in Thermoelectric-Bonded Materials Using Hypersingular Integral Equations. *Mathematics* **2023**, *11*, 3248. https://doi.org/10.3390/math11143248

Academic Editors: Hong Zheng and Hongyu LIU

Received: 4 June 2023
Revised: 5 July 2023
Accepted: 20 July 2023
Published: 24 July 2023

1. Introduction

The stability and safety of materials represent critical issues in engineering structures, where the presence of cracks may jeopardize the strength of materials. Many researchers have been drawn to investigate the stability behavior of structures or materials subject to remote stress by considering the types of materials such as infinite [1–3], finite [4,5], half plane [6–8], and bonded materials [9–13]. These types of materials have several conditions such as elasticity [14–16], thermoelasticity [17–19], magnetoelasticity [20–22], and electricity [23–25]. One of the important structures in manufacturing are thermoelectric

materials. When exposed to a temperature difference, these materials generate an electrical voltage. Cracks in thermoelectric materials can have a significant impact on their performance and durability, so it is critical to carefully control the manufacturing process and minimize crack formation to optimize their thermoelectric properties. Previous works utilized a variety of methods to investigate crack problems in thermoelectric materials subjected to remote stress.

Wang et al. [23] investigated the transient response of an arbitrarily located inner finite-size crack in thermoelectric materials using singularity integral equations based on the Fourier and Laplace transforms. Their investigation revealed that when the crack is positioned at the vertical center, there is an amplification of the field concentrations at the crack tip. Additionally, they observed that the electrical permeability of the crack exerts only a minor influence on the efficiency of energy conversion. By utilizing the complex function method and conformal mapping theory, Jiang et al. [24] successfully addressed a two-dimensional problem. Their study focused on the behavior of infinite thermoelectric materials, specifically a circular hole with two unequal cracks. The investigation considered the impact of uniform electric current and thermal flux on the system. It was determined that the variable of thermoelectric and stress intensity factors (SIFs) depends on the circular hole radius and lengths of cracks. According to Zheng and Gao [25], when the interior of the crack is filled with the same gas as at infinity, the applied electric field does not bear an effect on crack growth. They used the complex variable method to obtain explicit solutions for the complex potentials of a circular arc crack in an infinite electrostrictive solid under remote electric fields. Zhang and Wang [26] employed a complex variable method to solve the problem of a straight crack within a medium experiencing coupled thermoelectric effects under thermal–electric loads. Their investigation revealed that the electric flux intensity factor is influenced by the far-field electric flux loads, while the thermal flux intensity factor is determined by the applied total energy flux loads. Through the utilization of the complex variable method, Song et al. [27] investigated the SIFs pertaining to a crack in thermoelectric materials in a two-dimensional context. Their research revealed that the heat flow, electric current, and stress fields all exhibit the typical square-root singularity at the crack tip. Furthermore, they discovered that SIFs exhibit a linear relationship with the heat flux but a non-linear relationship with the electric current. The two-dimensional problem of an elliptic hole or a crack in a thermoelectric material subjected to uniform electric current density and energy flux at infinity was generalized by Zhang and Wang [28]. They used the complex variable method and the conformal mapping technique, and their results showed that the concentration factors of electric current density and stress at the hole rim increase as the value of the elliptic hole's major-to-minor axis ratio increase. Yu et al. [29] presented a rigorous solution to the Hilbert arc problem for a circular-arc crack problem in an infinite thermoelectric material subjected to electrical and thermal loading using the complex potentials function. They discovered that SIFs at crack tips are affected by the loading direction, electric conductivity, thermal conductivity, crack central angle, and thermoelastic isotropy. By employing the complex variable method and conformal mapping technique, Zhang et al. [30] successfully solved two-dimensional problems concerning a thermoelectric material containing either an elliptic hole or a rigid inclusion. These systems were subjected to uniform electric current density and energy flux at infinity. The researchers found that when an electric field is applied to the surface of a hole or rigid inclusion, the energy flux does not vanish due to the combined influence of the Joule heat and the Seebeck effect. Yu et al. [31] utilized complex potential functions and Cauchy integrals to solve the problem of a circular inhomogeneity embedded in thermoelectric materials subjected to uniform electric current density and energy flux. It was revealed that electrically and thermally induced stress has a linear relationship with the energy flux applied at infinity but a nonlinear relationship with the remote electric current density. Liu et al. [32] used the electric field saturation model to investigate the energy flux intensity factor, thermal flux intensity factor, and SIFs for a crack that is vertical to the applied electric flux and energy flux loads in thermoelectric materials. They discovered that all of

these intensity factors at the electrically yielded crack tips are independent of the strength and size of electrical saturation. Song et al. [33] analyzed the thermal SIFs at the crack tips of an interface crack subjected to a remote electric current in thermoelectric bonded materials using complex variable functions. They obtain that the electric current may either intensify fact neutralize the thermal SIFs depending on the bonded material parameters. Sladek et al. [34] used the finite element method with a collocation approach for kinematic constraints between strains and displacements to analyze the nano-sized crack problems in thermoelectric materials. They obtain the influence of the size effect on the variation of crack opening displacements to SIFs at crack tips. Cui et al. [35] proposed an analytical model to assess fatigue cracking and its impact on the power of a hybrid photovoltaic thermoelectric device. They discovered that combining a thermoelectric module and a photovoltaic cell with a low temperature coefficient can increase in total electric power. According to Jiang and Zhou [36], SIFs are affected by crack length, crack spacing, and the bi-elastic constant ratio for dual collinear interface cracks on the electric potential and temperature of thermoelectric-bonded materials subjected to electric and thermal loads. Moreover, they solved SIFs using Laplace equations and the driving forces of electric current density and energy flux. HSIEs are widely presented in different fields of physics and engineering such as crack problems in fracture mechanics because this method offers several advantages over other methods commonly used in crack analysis. These advantages include increased efficiency, flexibility in handling different crack types, accurate representation of crack tip behavior, and COD can be obtained from the solution of the equation directly [37–40]. Given these advantages, this method also has some limitations. It can be more complex to formulate and solve compared to simpler methods like the boundary element method. Additionally, they may require careful treatment of crack tip singularities and integration techniques to ensure accurate solutions. However, overall, HSIEs are a valuable tool in crack analysis and have contributed significantly to the understanding and prediction of crack behavior in various engineering applications.

To the best of the authors' knowledge, there is little information on the formulation of the multiple cracks problem in thermoelectric-bonded materials subjected to remote stress using HSIEs. The problem is formulated into HSIEs using the modified complex stress potential function method, with the help of continuity conditions of the resultant electric force and displacement electric function, and temperature and resultant heat flux are continuous across the bonded materials' interface. In addition, the findings obtained from this study can be valuable for engineers when investigating the stability behavior of bonded structures or materials exposed to electrical forces. By utilizing the obtained values of SIFs, engineers can gain insights into the stability of such structures or materials under these conditions. It provides engineers with an enhanced ability to predict crack behavior, enhance structural integrity, and design safer and more reliable engineering components and structures especially for thermoelectric-bonded materials. Furthermore, the formulation and investigation of crack problems have yielded substantial insights and comprehension in the field of fracture mechanics. This knowledge has played a pivotal role in predicting failures, optimizing designs, developing new materials, monitoring structural health, and conducting non-destructive evaluations. Consequently, these advancements have had a profound impact on various industries, enhancing safety measures and facilitating the creation of structures and materials that are more resilient and efficient.

2. Preliminary Knowledge

2.1. Thermoelectric Material

Bergman and Levy [41] have outlined that, in the absence of electric charges and heat sources, the governing equations for a thermoelectric material can be mathematically represented as:

$$\nabla \bullet \mathbf{J} = 0 \tag{1}$$

$$\nabla \bullet \mathbf{q} + \mathbf{J} \bullet \nabla V = 0 \tag{2}$$

$$\mathbf{J} = -\lambda \nabla V - \lambda \varepsilon \nabla T \tag{3}$$

$$\mathbf{q} = -\lambda \varepsilon T \nabla V - (\kappa + \lambda \varepsilon^2 T) \nabla T \tag{4}$$

where V is electric potential, T is absolute temperature, λ is electric conductivity, κ is thermal conductivity, ε is Seebeck coefficient, $\mathbf{J}$ is electric current density vector and $\mathbf{q}$ is heat flux vector. Since energy is transported by both electrons and heat, then the energy flux vector $\mathbf{U}$ can be derived from the electric current density and heat flux as

$$\mathbf{U} = \mathbf{q} + \mathbf{J}V. \tag{5}$$

According to Zhang and Wang [26], an analytic function F is defined as $F = V + \varepsilon T$, then we have

$$\mathbf{J} = -\lambda \nabla F \tag{6}$$

$$\mathbf{U} = -\lambda F \nabla F - \kappa \nabla T. \tag{7}$$

Combining Equations (1), (2), (6) and (7), the constitutive equations become

$$\nabla^2 F = 0 \tag{8}$$

$$\kappa \nabla^2 T + \lambda (\nabla F)^2 = 0. \tag{9}$$

For the two-dimensional thermoelectric problem considered here, the solutions of F and T can be expressed as,

$$F = \mathrm{Re}[f(z)] \tag{10}$$

$$T = \mathrm{Re}[g(z)] - \frac{\lambda}{4\kappa} f(z)\overline{f(z)} \tag{11}$$

where $z = x + iy$, $f(z)$ and $g(z)$ are unknown analytic functions for electric and thermal fields, respectively, and "Re" stands for the real part of a complex number.

2.2. Complex Stress Potential Functions

According to Song et al. [33], the stresses $(\sigma_x, \sigma_y, \sigma_{xy})$, resultant electric force (X, Y) and displacements electric functions (u, v) induced by the thermoelectric function can be obtained as follows

$$\sigma_x + \sigma_y = 2[\phi'(z) + \overline{\psi'(z)}] + \frac{E\alpha\lambda}{\kappa} f(z)\overline{f(z)} \tag{12}$$

$$\sigma_y - \sigma_x + 2i\sigma_{xy} = 2[\bar{z}\phi''(z) + \psi'(z)] + \frac{E\alpha\lambda}{\kappa} f'(z)\overline{F(z)} \tag{13}$$

$$-Y + iX = \phi(z) + z\overline{\phi'(z)} + \overline{\psi(z)} + \frac{E\alpha\lambda}{4G\kappa} F(z)\overline{f(z)} \tag{14}$$

$$u + iv = \frac{1}{2G}[K\phi(z) - z\overline{\phi'(z)} - \overline{\psi(z)}] + \alpha \int \Omega(z)dz - \frac{E\alpha\lambda}{4G\kappa} F(z)\overline{f(z)} \tag{15}$$

where $\phi(z)$ and $\psi(z)$ are complex stress potential functions, G is shear modulus, $K = (3 - \mu)/(1 + \mu)$, μ is Poisson's ratio, E is Young's modulus, α is the coefficient of thermal expansion, $\Omega(z) = -(\lambda/\kappa) f(z)^2 + (2/\kappa) g(z)$, and $F(z) = \int f(z)dz$.

The derivative in a specified direction of resultant force Function (14) with respect to z yields the normal (N) and tangential (T) components of traction along the segment $\overline{z, z + dz}$, where $d\bar{z}/dz = -e^{-2i\theta}$ and θ is the tangential angle to the crack as follows

$$\frac{d}{dz}\{-Y + iX\} = \phi'(z) + \overline{\phi'(z)} + \frac{d\bar{z}}{dz}\left(z\overline{\phi''(z)} + \overline{\psi'(z)}\right) + \frac{E\alpha\lambda}{4G\kappa}\left(f(z)\overline{f(z)} + F(z)\overline{f'(z)}\frac{d\bar{z}}{dz}\right) = N + iT. \tag{16}$$

Note that the traction $N + iT$ depends on the position of point z and the direction of the segment $d\bar{z}/dz$.

According to Nik Long and Eshkuvatov [1] and Song et al. [33], the complex stress potential functions, and unknown analytic functions for electric and thermal fields in the case of a crack in an infinite material can be expressed by

$$\begin{aligned}
\phi(z) &= \frac{1}{2\pi}\int_L \frac{g(t)dt}{t-z} \\
\psi(z) &= \frac{1}{2\pi}\int_L \frac{\overline{g(t)}dt}{t-z} + \frac{1}{2\pi}\int_L g(t)\left(\frac{d\bar{t}}{t-z} - \frac{\bar{t}dt}{(t-z)^2}\right) \\
f(z) &= \frac{i\mathbf{J}}{2\lambda}\sqrt{z^2-a^2} \\
F(z) &= \frac{i\mathbf{J}}{4\lambda}\left(z\sqrt{z^2-a^2} - a^2\ln(z+\sqrt{z^2-a^2})\right) \\
g(z) &= \frac{i\mathbf{U}}{2}\sqrt{z^2-a^2} \\
\Omega(z) &= \frac{\mathbf{J}^2}{4\lambda\kappa}(z^2-a^2) + \frac{i\mathbf{U}}{\kappa}\sqrt{z^2-a^2}
\end{aligned} \tag{17}$$

where $2a$ is the length of the crack and $g(t)$ is the crack opening displacement (COD) function defined as

$$g(t) = \frac{2G}{i(K+1)}\Big[(u(t)+iv(t))^+ - (u(t)+iv(t))^-\Big],\ (t \in L) \tag{18}$$

$(u(t)+iv(t))^+$ and $(u(t)+iv(t))^-$ denote the displacements at a point t of the upper and lower crack faces, respectively. Note that the COD function has the following properties

$$g(t) = O\left[\sqrt{t-t_{A_j}}\right] \qquad \text{at the crack tip } A_j,$$

where $j = 1, 2$.

3. Thermoelectric-Bonded Materials

3.1. Modified Complex Stress Potential Function

Consider two cracks that lie in both the upper and lower parts of thermoelectric-bonded materials subjected to remote stress, as shown in Figure 1. The modified complex stress potential functions were discussed by Chen and Hasebe [42]. The crack L_1 lies in the upper part of thermoelectric-bonded materials and can be expressed by:

$$\phi_1(z) = \phi_{1p}(z) + \phi_{1c}(z), \qquad \psi_1(z) = \psi_{1p}(z) + \psi_{1c}(z) \tag{19}$$

where $\phi_{1p}(z)$ and $\psi_{1p}(z)$ are the principal part of the complex stress potential functions and the elementary solution for isotropic medium (infinite materials), whereas $\phi_{1c}(z)$ and $\psi_{1c}(z)$ are the complement part of the complex stress potential functions. The complex stress potential functions for the crack L_2 lie in the lower part of thermoelectric-bonded materials represented by $\phi_2(z)$ and $\psi_2(z)$. The continuity condition of the resultant electric force (14) is defined as follows.

$$[-Y+iX]^+ = [-Y+iX]^-,$$

$$\left[\phi_1(t) + t\overline{\phi_1'(t)} + \overline{\psi_1(t)} + \frac{E_1\alpha_1\lambda_1}{4G_1\kappa_1}F_1(t)\overline{f_1(t)}\right]^+ = \left[\phi_2(t) + t\overline{\phi_2'(t)} + \overline{\psi_2(t)} + \frac{E_2\alpha_2\lambda_2}{4G_2\kappa_2}F_2(t)\overline{f_2(t)}\right]^-$$

Applying the modified complex stress potential Functions (19) then yields:

$$\left[\phi_{1p}(t)+\phi_{1c}(t)+t\overline{\phi'_{1p}(t)}+\overline{\psi_{1p}(t)}+t\overline{\phi'_{1c}(t)}+\overline{\psi_{1c}(t)}+\frac{E_1\alpha_1\lambda_1}{4G_1\kappa_1}\left(F_{1p}(t)\overline{f_{1p}(t)}+F_{1c}(t)\overline{f_{1c}(t)}\right)\right]^+$$
$$=\left[\phi_2(t)+t\overline{\phi'_2(t)}+\overline{\psi_2(t)}+\frac{E_2\alpha_2\lambda_2}{4G_2\kappa_2}F_2(t)\overline{f_2(t)}\right]^- . \quad (20)$$

Whereas the continuity condition of displacement electric Function (15) is defined as follows:

$$[u+iv]^+=[u+iv]^-,$$
$$\left[\frac{1}{2G_1}[K_1\phi_1(t)-t\overline{\phi'_1(t)}-\overline{\psi_1(t)}]+\alpha_1\int\Omega_1(t)dt-\frac{E_1\alpha_1\lambda_1}{4G_1\kappa_1}F_1(t)\overline{f_1(t)}\right]^+$$
$$=\left[\frac{1}{2G_2}[K_2\phi_2(t)-t\overline{\phi'_2(t)}-\overline{\psi_2(t)}]+\alpha_2\int\Omega_2(t)dt-\frac{E_2\alpha_2\lambda_2}{4G_2\kappa_2}F_2(t)\overline{f_2(t)}\right]^-$$

Applying the modified complex stress potential Functions (19) then yields:

$$G_2\left[K_1\phi_{1p}(t)+K_1\phi_{1c}(t)-\left(t\overline{\phi'_{1p}(t)}+\overline{\psi_{1p}(t)}\right)-\left(t\overline{\phi'_{1c}(t)}+\overline{\psi_{1c}(t)}\right)+2G_1\alpha_1\left(\int\Omega_{1p}(t)dt+\int\Omega_{1c}(t)dt\right)\right.$$
$$\left.-\frac{E_1\alpha_1\lambda_1}{2\kappa_1}\left(F_{1p}(t)\overline{f_{1p}(t)}+F_{1c}(t)\overline{f_{1c}(t)}\right)\right]^+$$
$$=G_1\left[K_2\phi_2(t)-t\overline{\phi'_2(t)}-\overline{\psi_2(t)}+2G_2\alpha_2\int\Omega_2(t)dt-\frac{E_2\alpha_2\lambda_2}{2\kappa_2}F_2(t)\overline{f_2(t)}\right]^- . \quad (21)$$

Note that $t\in L_j$, $(j=1,2)$ along the crack interface, and the $+$ and $-$ signs represent the upper and lower parts of thermoelectric-bonded materials, respectively.

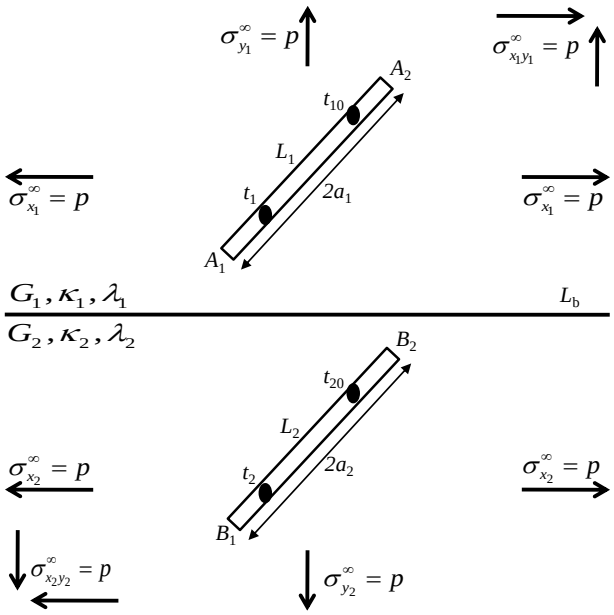

Figure 1. Two cracks L_1 and L_2 in thermoelectric-bonded materials subjected to remote stress.

For problems involving steady-state electric conduction in two dimensions, the temperature functions associated with bonded materials can be derived by utilizing two complex potentials, namely $f_1(z)$ and $f_2(z)$. These potentials satisfy the Laplace equation in the respective upper and lower parts. To establish the boundary conditions, the complex potentials are employed to express the resultant heat flux Q_j and temperature T_j for each medium. The formulations for these quantities are provided as follows

$$f_j(z) = T_j(x,y) + iQ_j(x,y)$$

$$Q_j = \int (q_{xj}dy - q_{yj}dx) = -\lambda_j \mathrm{Im}[f_j(z)] \tag{22}$$

$$T_j = \mathrm{Re}[f_j(z)] \tag{23}$$

In the given context, the quantities q_{xj} and q_{yj} represent the heat flux components in the x and y directions, respectively. Additionally, λ_j denotes the electric conductivity, where $j = 1$ for the upper part and $j = 2$ for the lower part.

If there exists a crack L in the upper part of the thermoelectric-bonded materials, it is convenient to express the electric complex potential $f_1(z)$ as

$$f_1(z) = f_{1p}(z) + f_{1c}(z) \tag{24}$$

where f_{1p} and f_{1c} are the principal and complementary parts of the electric complex function, respectively. Since the temperature and resultant heat flux are continuous across the crack bonded materials interface, it implies:

$$[f_1(t) + \overline{f_1(t)}]^+ = [f_2(t) + \overline{f_2(t)}]^-, t \in L \tag{25}$$

$$\lambda_1[f_1(t) - \overline{f_1(t)}]^+ = \lambda_2[f_2(t) - \overline{f_2(t)}]^-, t \in L \tag{26}$$

where a bar is used to indicate a conjugate complex quantity, while superscripts $+$ and $-$ are used for the boundary values of the temperature potentials for the upper and lower parts, respectively. Substituting Equation (24) into Equations (25) and (26), then it is satisfied by the following complex potentials:

$$[f_{1p}(t) + f_{1c}(t) + \overline{f_{1p}(t)} + \overline{f_{1c}(t)}]^+ = [f_2(t) + \overline{f_2(t)}]^- \tag{27}$$

$$\lambda_1[f_{1p}(t) + f_{1c}(t) - \overline{f_{1p}(t)} - \overline{f_{1c}(t)}]^+ = \lambda_2[f_2(t) - \overline{f_2(t)}]^-. \tag{28}$$

Applying analytical continuation to Equations (27) and (28), the following expressions are obtainable:

$$f_{1c}(z) = \frac{\lambda_1 - \lambda_2}{\lambda_1 + \lambda_2}\overline{f_{1p}}(z), \quad z \in S_1 + L_b \tag{29}$$

$$f_2(z) = \frac{2\lambda_1}{\lambda_1 + \lambda_2} f_{1p}(z), \quad z \in S_2 + L_b. \tag{30}$$

Once the principle part of the complex potentials, $f_{1p}(z)$, is determined, the electric functions associated with the thermoelectric-bonded materials' problem can be obtained. Similar to the thermal complex potentials function, it yields:

$$g_{1c}(z) = \frac{\kappa_1 - \kappa_2}{\kappa_1 + \kappa_2}\overline{g_{1p}}(z), \quad z \in S_1 + L_b \tag{31}$$

$$g_2(z) = \frac{2\kappa_1}{\kappa_1 + \kappa_2} g_{1p}(z), \quad z \in S_2 + L_b. \tag{32}$$

Note that L_b is the boundary of thermoelectric-bonded materials, S_1 and S_2 are the upper and lower parts of thermoelectric bonded materials, respectively. Applying analytical continuation to Equations (20) and (21), and substituted with Equations (29)–(32) the following expressions are obtainable:

$$\phi_{1c}(z) = \Gamma_1\left(z\overline{\phi'_{1p}}(z) + \overline{\psi_{1p}}(z)\right) + \Gamma_2\overline{F_{1p}}(z)f_{1p}(z) + \Gamma_3\int \overline{f_{1p}}^2(z)dz - \Gamma_4\int \overline{g_{1p}}(z)dz \tag{33}$$

$$\psi_{1c}(z) = \Gamma_5\overline{\phi_{1p}}(z) - z\phi'_{1c}(z) + \Gamma_6\overline{F_{1p}}(z)f_{1p}(z) + \Gamma_7\int \overline{\Omega_{1p}}(z)dz + \Gamma_8\int \overline{f_{1p}}^2(z)dz - \Gamma_9\int \overline{g_{1p}}(z)dz \tag{34}$$

$$\phi_2(z) = \Gamma_{10}\phi_{1p}(z) + \Gamma_{11}F_{1p}(z)\overline{f_{1p}}(z) + \Gamma_{12}F_{1p}(z)\overline{f_{1p}}(z) + \Gamma_7\int \Omega_{1p}(z)dz + \Gamma_8\int f_{1p}^2(z)dz - \Gamma_9\int g_{1p}(z)dz \tag{35}$$

$$\psi_2(z) = \Gamma_{13}\left(z\phi'_{1p}(z) + \psi_{1p}(z)\right) - z\phi'_2(z) + \Gamma_{14}F_{1p}(z)\overline{f_{1p}}(z) + \Gamma_{15}\int f_{1p}^2(z)dz - \Gamma_{16}\int g_{1p}(z)dz \tag{36}$$

where $\overline{\phi_{1p}}(z) = \overline{\phi_{1p}(\bar{z})}$, and Γ_j are bi-elastic constants ratio defined as

$$\Gamma_1 = \frac{G_2 - G_1}{G_1 + G_2K_1},\quad \Gamma_2 = \frac{(2G_2-1)E_1\alpha_1\lambda_1}{4\kappa_1(G_1+G_2K_1)}\left(\frac{\lambda_1-\lambda_2}{\lambda_1+\lambda_2}\right)^2,\quad \Gamma_3 = \frac{2G_1G_2\alpha_1\lambda_1}{\kappa_1\left(G_1+G_2\kappa_1\right)}\left(\frac{\lambda_1-\lambda_2}{\lambda_1+\lambda_2}\right)^2,$$

$$\Gamma_4 = \frac{4G_1G_2\alpha_1}{\kappa_1\left(G_1+G_2\kappa_1\right)}\left(\frac{\kappa_1-\kappa_2}{\kappa_1+\kappa_2}\right),\quad \Gamma_5 = \frac{G_2K_1 - G_1K_2}{G_1K_2+G_2},\quad \Gamma_6 = \left(\frac{E_2\alpha_2\lambda_2(2G_1G_2+G_1K_2)}{4G_2\kappa_2(G_1K_2+G_2)}\right)\left(\frac{2\lambda_1}{\lambda_1+\lambda_2}\right)^2,$$

$$\Gamma_7 = \frac{2G_1G_2\alpha_1}{\left(G_1K_2+G_2\right)},\quad \Gamma_8 = \frac{2G_1G_2\alpha_2\lambda_2}{\kappa_2\left(G_1K_2+G_2\right)}\left(\frac{2\lambda_1}{\lambda_1+\lambda_2}\right)^2,\quad \Gamma_9 = \frac{8G_1G_2\alpha_2\kappa_1}{\kappa_2(\kappa_1+\kappa_2)\left(G_1K_2+G_2\right)},$$

$$\Gamma_{10} = \frac{(K_1+1)G_2}{G_1K_2+G_2},\quad \Gamma_{11} = \frac{E_2\alpha_2\lambda_2(2G_1-1)}{4\kappa_2(G_1K_2+G_2)}\left(\frac{2\lambda_1}{\lambda_1+\lambda_2}\right)^2,\quad \Gamma_{12} = \frac{G_2E_1\alpha_1\lambda_1(1-2G_1)}{4G_1\kappa_1(G_1K_2+G_2)},$$

$$\Gamma_{13} = \frac{G_2(1+K_1)}{G_1+G_2K_1},\quad \Gamma_{14} = \frac{(K_1+2G_1)G_2E_1\alpha_1\lambda_1}{4G_1\kappa_1(G_1+G_2K_1)}\left(\frac{\lambda_1-\lambda_2}{\lambda_1+\lambda_2}\right)^2,\quad \Gamma_{15} = \frac{2G_1G_2\alpha_1\lambda_1}{\kappa_1\left(G_1+G_2K_1\right)}\left(\frac{\lambda_1-\lambda_2}{\lambda_1+\lambda_2}\right)^2,$$

$$\Gamma_{16} = \frac{4G_1G_2\alpha_1}{\kappa_1\left(G_1+G_2K_1\right)}\left(\frac{\kappa_1-\kappa_2}{\kappa_1+\kappa_2}\right)$$

3.2. HSIEs for a Crack in the Upper Part of Thermoelectric-Bonded Materials

Consider a crack L with length $2a$ that lies in the upper part of thermoelectric-bonded materials subjected to remote stress, as shown in Figure 2.

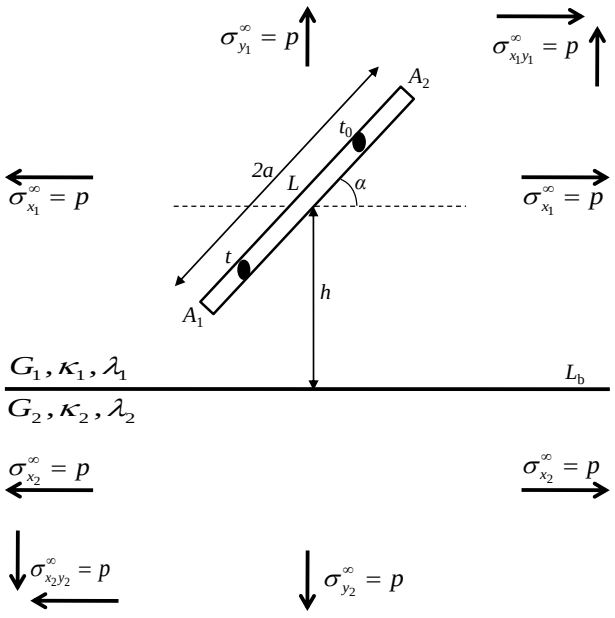

Figure 2. A crack L in the upper part of thermoelectric-bonded materials subjected to remote stress.

In order to formulate the HSIEs for a crack in the upper part of thermoelectric-bonded materials, we need to define two traction components which are $[N(t_0)+iT(t_0)]_{1p}$ and $[N(t_0)+iT(t_0)]_{1c}$ for the principle and complementary parts, respectively. These traction components are obtained when the observation point is placed at the point, t_0 ($t_0 \in L$), caused by COD function $g(t)$ at $t \in L$, which gives:

$$[N(t_0)+iT(t_0)]_1 = [N(t_0)+iT(t_0)]_{1p} + [N(t_0)+iT(t_0)]_{1c}. \tag{37}$$

To obtain the principal part $[N(t_0)+iT(t_0)]_{1p}$, substitute Equation (17) into Equation (16), then let point z approach t_0 on the crack and change $d\bar{z}/dz$ into $d\bar{t}_0/dt_0$. Meanwhile, to obtain the complementary part $[N(t_0)+iT(t_0)]_{1c}$, substitute Equations (33) and (34) into Equation (16), and then apply Equation (17). The sum between these two parts then represents the HSIEs as follows:

$$[N(t_0)+iT(t_0)]_1 = \frac{1}{\pi}\oint_L \frac{g(t)dt}{(t-t_0)^2} + \frac{1}{2\pi}\int_L M_1(t,t_0)g(t)dt + \frac{1}{2\pi}\int_L M_2(t,t_0)\overline{g(t)}dt + M_3(a,t_0) \tag{38}$$

where

$$\begin{aligned}
M_1(t,t_0) = &-\frac{1}{(t-t_0)^2} + \frac{1}{(\bar{t}-\bar{t}_0)^2}\frac{d\bar{t}}{dt}\frac{d\bar{t}_0}{dt_0} + \Gamma_1\left[\frac{1}{(t-\bar{t}_0)^2} + \frac{2(\bar{t}_0-\bar{t})}{(t-\bar{t}_0)^3} + \left(\frac{1}{(\bar{t}-t_0)^2} + \frac{1}{(t-\bar{t}_0)^2}\right)\frac{d\bar{t}}{dt}\right.\\
&\left. + \left(\frac{2(2t_0-3\bar{t}_0+\bar{t})}{(t-\bar{t}_0)^3} - \frac{6(\bar{t}_0-\bar{t})(\bar{t}_0-t_0)}{(t-\bar{t}_0)^4} - \left(\frac{1}{(t-\bar{t}_0)^2} + \frac{2(\bar{t}_0-t_0)}{(t-\bar{t}_0)^3}\right)\frac{d\bar{t}}{dt} - \frac{1}{(t-\bar{t}_0)^2}\right)\frac{d\bar{t}_0}{dt_0}\right]\\
&+ \Gamma_5\frac{1}{(t-\bar{t}_0)^2}\frac{d\bar{t}_0}{dt_0}\\
M_2(t,t_0) = &\frac{1}{(\bar{t}-\bar{t}_0)^2}\frac{d\bar{t}}{dt} + \left(\frac{1}{(\bar{t}-\bar{t}_0)^2} + \frac{2(t_0-t)}{(\bar{t}-\bar{t}_0)^3}\frac{d\bar{t}}{dt}\right)\frac{d\bar{t}_0}{dt_0} + \Gamma_1\left[\frac{1}{(\bar{t}-t_0)^2} + \frac{1}{(t-\bar{t}_0)^2}\right.\\
&\left. + \left(\frac{1}{(\bar{t}-t_0)^2} + \frac{2(t_0-t)}{(\bar{t}-t_0)^3}\right)\frac{d\bar{t}}{dt} + \left(\frac{2(t_0-\bar{t}_0)}{(t-\bar{t}_0)^3} - \frac{1}{(t-\bar{t}_0)^2}\right)\frac{d\bar{t}_0}{dt_0}\right]
\end{aligned}$$

$$\begin{aligned}
M_3(a,t_0) = &\Gamma_2\frac{\mathbf{J}^2}{4\lambda_1^2}\left(t_0^2-a^2+\frac{t_0}{2\sqrt{t_0^2-a^2}}\left(t_0\sqrt{t_0^2-a^2}-a^2\ln(t_0+\sqrt{t_0^2-a^2})\right)\right)\\
&+\left(\Gamma_2+(\Gamma_6-\Gamma_2)\frac{d\bar{t}_0}{dt_0}\right)\frac{\mathbf{J}^2}{4\lambda_1^2}\left(\bar{t}_0^2-a^2+\frac{\bar{t}_0}{2\sqrt{\bar{t}_0^2-a^2}}\left(\bar{t}_0\sqrt{\bar{t}_0^2-a^2}-a^2\ln(\bar{t}_0+\sqrt{\bar{t}_0^2-a^2})\right)\right)\\
&+\Gamma_2\frac{\mathbf{J}^2}{4\lambda_1^2}(t_0-\bar{t}_0)\left(3\bar{t}_0+\left(\bar{t}_0\sqrt{\bar{t}_0^2-a^2}-a^2\ln(\bar{t}_0+\sqrt{\bar{t}_0^2-a^2})\right)\frac{(\bar{t}_0^2-\bar{t}_0-a^2)}{2\left(\sqrt{\bar{t}_0^2-a^2}\right)^3}\right)\frac{d\bar{t}_0}{dt_0}\\
&+\Gamma_3\frac{\mathbf{J}^2}{4\lambda_1^2}\left(2a^2-t_0^2-\bar{t}_0^2+(3\bar{t}_0^2-2t_0\bar{t}_0-a^2)\frac{d\bar{t}_0}{dt_0}\right)+\Gamma_4\frac{i\mathbf{U}}{2}\left(\sqrt{t_0^2-a^2}-\sqrt{\bar{t}_0^2-a^2}+\frac{2\bar{t}_0^2-\bar{t}_0t_0-a^2}{\sqrt{\bar{t}_0^2-a^2}}\frac{d\bar{t}_0}{dt_0}\right)\\
&+\left[\left(\frac{\Gamma_7}{\kappa_1}-\frac{\Gamma_8}{\lambda_1}\right)\frac{\mathbf{J}^2}{4\lambda_1}(\bar{t}_0^2-a^2)+\left(\frac{\Gamma_7}{\kappa_1}-\frac{\Gamma_9}{2}\right)i\mathbf{U}\sqrt{\bar{t}_0^2-a^2}\right]\frac{d\bar{t}_0}{dt_0}\\
&+(\Gamma_{17}+\Gamma_{18})\frac{\mathbf{J}^2}{4\lambda_1^2}\left[\sqrt{t_0^2-a^2}\sqrt{\bar{t}_0^2-a^2}+\left(t_0\sqrt{t_0^2-a^2}-a^2\ln(t_0+\sqrt{t_0^2-a^2})\right)\frac{\bar{t}_0}{2\sqrt{\bar{t}_0^2-a^2}}\frac{d\bar{t}_0}{dt_0}\right]
\end{aligned}$$

and

$$\Gamma_{17} = \frac{E_1\alpha_1\lambda_1}{4G_1\kappa_1}, \qquad \Gamma_{18} = \frac{E_1\alpha_1\lambda_1}{4G_1\kappa_1}\left(\frac{\kappa_1-\kappa_2}{\kappa_1+\kappa_2}\right)^2.$$

Note that the first integral with the equal sign in Equation (38) represents the hypersingular integral and must be defined as a finite part integral. If $G_1 = G_2$, $K_1 = K_2$, and

$E_1 = E_2$, and the values of $\alpha_1 = \alpha_2 = 0$ and $\lambda_1 = \lambda_2 = 0$, then Equation (38) reduces to HSIEs for a crack in an infinite material as follows [1,9]:

$$[N(t_0) + iT(t_0)]_1 = \frac{1}{\pi} \neq_L \frac{g(t)dt}{(t-t_0)^2} + \frac{1}{2\pi} \int_L \frac{1}{(t-t_0)^2} \left(\frac{(t-t_0)^2}{(\bar{t}-\bar{t}_0)^2} \frac{d\bar{t}}{dt} \frac{d\bar{t}_0}{dt_0} - 1 \right) g(t)dt + \frac{1}{2\pi} \int_L \frac{t-t_0}{(\bar{t}-\bar{t}_0)^3} \left(\frac{\bar{t}-\bar{t}_0}{t-t_0} \left(\frac{d\bar{t}}{dt} + \frac{d\bar{t}_0}{dt_0} \right) - 2\frac{d\bar{t}}{dt} \frac{d\bar{t}_0}{dt_0} \right) \overline{g(t)}dt \quad (39)$$

If $G_2 = 0$, and the values of $\alpha_1 = \alpha_2 = 0$, $\lambda_1 = \lambda_2 = 0$ and $\kappa_2 = 0$, then Equation (38) reduces to HSIEs for a crack in half-plane materials as follows [6,43]

$$\begin{aligned}[N(t_0) + iT(t_0)]_1 = {} & \frac{1}{\pi} \neq_L \frac{g(t)dt}{(t-t_0)^2} + \frac{1}{2\pi} \int_L \left[-\frac{1}{(t-t_0)^2} - \frac{1}{(t-\bar{t}_0)^2} - \frac{2(\bar{t}_0-\bar{t})}{(t-\bar{t}_0)^3} + \frac{1}{(\bar{t}-\bar{t}_0)^2} \frac{d\bar{t}}{dt} \frac{d\bar{t}_0}{dt_0} \right. \\ & - \left(\frac{1}{(t-\bar{t}_0)^2} + \frac{1}{(\bar{t}-t_0)^2} \right) \frac{d\bar{t}}{dt} + \left(\frac{2(3\bar{t}_0 - 2t_0 - \bar{t})}{(t-\bar{t}_0)^3} + \frac{6(\bar{t}_0-\bar{t})(\bar{t}_0-t_0)}{(t-\bar{t}_0)^4} \right) \frac{d\bar{t}_0}{dt_0} \\ & \left. + \left(\frac{1}{(t-\bar{t}_0)^2} + \frac{2(\bar{t}_0-t_0)}{(t-\bar{t}_0)^3} \right) \frac{d\bar{t}}{dt} \frac{d\bar{t}_0}{dt_0} \right] g(t)dt + \frac{1}{2\pi} \int_L \left[-\frac{1}{(\bar{t}-\bar{t}_0)^2} - \frac{1}{(t-\bar{t}_0)^2} \right. \\ & + \left(\frac{1}{(\bar{t}-\bar{t}_0)^2} - \frac{1}{(\bar{t}-t_0)^2} - \frac{2(t_0-t)}{(\bar{t}-t_0)^3} \right) \frac{d\bar{t}}{dt} + \left(\frac{1}{(\bar{t}-\bar{t}_0)^2} + \frac{1}{(t-\bar{t}_0)^2} + \frac{2(\bar{t}_0-t_0)}{(t-\bar{t}_0)^3} \right. \\ & \left. \left. + \frac{2(t_0-t)}{(\bar{t}-\bar{t}_0)^3} \frac{d\bar{t}}{dt} \right) \frac{d\bar{t}_0}{dt_0} \right] \overline{g(t)}dt \end{aligned} \quad (40)$$

Therefore, if $G_1 = G_2$, $K_1 = K_2$, and $E_1 = E_2$, and the values of $\alpha_1 = \alpha_2$, $\lambda_1 = \lambda_2$ and $\kappa_1 = \kappa_2$, then Equation (38) reduces to HSIEs for a crack in an infinite thermoelectric material as follows:

$$[N(t_0) + iT(t_0)]_1 = \frac{1}{\pi} \neq_L \frac{g(t)dt}{(t-t_0)^2} + \frac{1}{2\pi} \int_L D_1(t,t_0) g(t)dt + \frac{1}{2\pi} \int_L D_2(t,t_0) \overline{g(t)}dt + D_3(a,t_0) \quad (41)$$

where

$$\begin{aligned} D_1(t,t_0) &= -\frac{1}{(t-t_0)^2} + \frac{1}{(\bar{t}-\bar{t}_0)^2} \frac{d\bar{t}}{dt} \frac{d\bar{t}_0}{dt_0} \\ D_2(t,t_0) &= \frac{1}{(\bar{t}-\bar{t}_0)^2} \frac{d\bar{t}}{dt} + \left(\frac{1}{(\bar{t}-\bar{t}_0)^2} + \frac{2(t_0-t)}{(\bar{t}-\bar{t}_0)^3} \frac{d\bar{t}}{dt} \right) \frac{d\bar{t}_0}{dt_0} \\ D_3(a,t_0) &= \frac{\mathbf{J}^2 E_1 \alpha_1 \lambda_1 (2G_1 + K_1)}{16 G_1 \kappa_1 \lambda_1^2 (K_1+1)} \left(\bar{t}_0^2 - a^2 + \frac{\bar{t}_0}{2\sqrt{\bar{t}_0^2 - a^2}} (\bar{t}_0 \sqrt{\bar{t}_0^2 - a^2} - a^2 \ln(\bar{t}_0 + \sqrt{\bar{t}_0^2 - a^2})) \right) \frac{d\bar{t}_0}{dt_0} \\ &\quad + \left[\left(\frac{2G_1\alpha_1}{\kappa_1(K_1+G_1)} - \frac{2G_1\alpha_1\lambda_1}{\kappa_1\lambda_1(K_1+1)} \right) \frac{\mathbf{J}^2}{4\lambda_1} (\bar{t}_0^2 - a^2) + \left(\frac{2G_1\alpha_1}{\kappa_1(K_1+G_1)} - \frac{2G_1\alpha_1}{\kappa_1(K_1+1)} \right) i\mathbf{U} \sqrt{\bar{t}_0^2 - a^2} \right] \frac{d\bar{t}_0}{dt_0} \\ &\quad + \frac{\mathbf{J}^2 E_1 \alpha_1 \lambda_1}{16 G_1 \kappa_1 \lambda_1^2} \left[\sqrt{t_0^2 - a^2} \sqrt{\bar{t}_0^2 - a^2} + \left(\frac{\bar{t}_0}{2\sqrt{\bar{t}_0^2 - a^2}} (t_0 \sqrt{t_0^2 - a^2} - a^2 \ln(t_0 + \sqrt{t_0^2 - a^2})) \right) \frac{d\bar{t}_0}{dt_0} \right] \end{aligned}$$

Whereas, if $G_2 = 0$ and the values of $\alpha_2 = 0$, $\lambda_2 = 0$, and $\kappa_2 = 0$, then Equation (38) reduces to HSIEs for a crack in half-plane thermoelectric materials as follows:

$$[N(t_0) + iT(t_0)]_1 = \frac{1}{\pi} \neq_L \frac{g(t)dt}{(t-t_0)^2} + \frac{1}{2\pi} \int_L W_1(t,t_0) g(t)dt + \frac{1}{2\pi} \int_L W_2(t,t_0) \overline{g(t)}dt + W_3(a,t_0) \quad (42)$$

where

$$W_1(t,t_0) = -\frac{1}{(t-t_0)^2} - \frac{1}{(t-\bar{t}_0)^2} - \frac{2(\bar{t}_0-\bar{t})}{(t-\bar{t}_0)^3} + \frac{1}{(\bar{t}-\bar{t}_0)^2}\frac{d\bar{t}}{dt}\frac{d\bar{t}_0}{dt_0} - \left(\frac{1}{(t-\bar{t}_0)^2} + \frac{1}{(\bar{t}-t_0)^2}\right)\frac{d\bar{t}}{dt}$$
$$+ \left(\frac{2(3\bar{t}_0-2t_0-\bar{t})}{(t-\bar{t}_0)^3} + \frac{6(\bar{t}_0-\bar{t})(\bar{t}_0-t_0)}{(t-\bar{t}_0)^4}\right)\frac{d\bar{t}_0}{dt_0} + \left(\frac{1}{(t-\bar{t}_0)^2} + \frac{2(\bar{t}_0-t_0)}{(t-\bar{t}_0)^3}\right)\frac{d\bar{t}}{dt}\frac{d\bar{t}_0}{dt_0}$$
$$W_2(t,t_0) = -\frac{1}{(\bar{t}-t_0)^2} - \frac{1}{(t-\bar{t}_0)^2}\frac{1}{(\bar{t}-\bar{t}_0)^2}\frac{d\bar{t}}{dt} + \left(\frac{1}{(\bar{t}-\bar{t}_0)^2} + \frac{2(t_0-t)}{(\bar{t}-\bar{t}_0)^3}\frac{d\bar{t}}{dt}\right)\frac{d\bar{t}_0}{dt_0}$$
$$- \left(\frac{1}{(\bar{t}-t_0)^2} + \frac{2(t_0-t)}{(\bar{t}-t_0)^3}\right)\frac{d\bar{t}}{dt} + \left(\frac{1}{(t-\bar{t}_0)^2} + \frac{2(\bar{t}_0-t_0)}{(t-\bar{t}_0)^3}\right)\frac{d\bar{t}_0}{dt_0}$$
$$W_3(a,t_0) = -\frac{\mathbf{J}^2E_1\alpha_1\lambda_1}{16\kappa_1\lambda_1^2G_1}\left[t_0^2 - a^2 + \frac{t_0}{2\sqrt{t_0^2-a^2}}\left(t_0\sqrt{t_0^2-a^2} - a^2\ln(t_0+\sqrt{t_0^2-a^2})\right)\right.$$
$$- \left(\bar{t}_0^2 - a^2 + \frac{\bar{t}_0}{2\sqrt{\bar{t}_0^2-a^2}}\left(\bar{t}_0\sqrt{\bar{t}_0^2-a^2} - a^2\ln(\bar{t}_0+\sqrt{\bar{t}_0^2-a^2})\right)\right)\left(\frac{d\bar{t}_0}{dt_0} - 1\right)$$
$$+ (t_0-\bar{t}_0)\left(3\bar{t}_0 + \left(\bar{t}_0\sqrt{\bar{t}_0^2-a^2} - a^2\ln(\bar{t}_0+\sqrt{\bar{t}_0^2-a^2})\right)\frac{(\bar{t}_0^2-\bar{t}_0-a^2)}{2\left(\sqrt{\bar{t}_0^2-a^2}\right)^3}\right)\frac{d\bar{t}_0}{dt_0}$$
$$\left. - \frac{1}{2}\sqrt{t_0^2-a^2}\sqrt{\bar{t}_0^2-a^2} - \left(\frac{\bar{t}_0}{4\sqrt{\bar{t}_0^2-a^2}}\left(t_0\sqrt{t_0^2-a^2} - a^2\ln(t_0+\sqrt{t_0^2-a^2})\right)\right)\frac{d\bar{t}_0}{dt_0}\right]$$

3.3. HSIEs for Multiple Cracks in the Upper Part of Thermoelectric-Bonded Materials

Consider two cracks, L_1 and L_2, in the upper part of thermoelectric-bonded materials subjected to remote stress as shown in Figure 3.

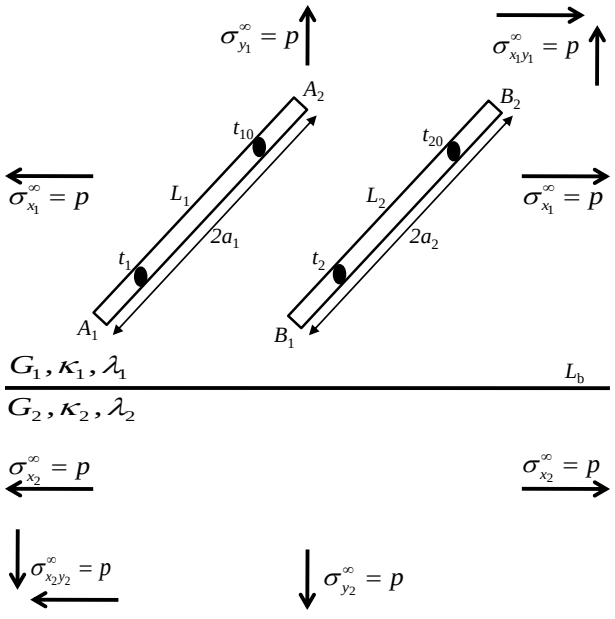

Figure 3. Two cracks L_1 and L_2 in the upper part of thermoelectric-bonded materials subjected to remote stress.

In order to formulate the HSIEs for two cracks in the upper part of thermoelectric-bonded materials, we need to define two groups of $N + iT$ which consist of four traction components $[N(t_{10}) + iT(t_{10})]_{11}$, $[N(t_{10}) + iT(t_{10})]_{12}$, $[N(t_{20}) + iT(t_{20})]_{22}$ and $[N(t_{20}) + iT(t_{20})]_{21}$ by using Equation (16). By then using the superposition principle, we can obtain the HSIEs for two cracks in the upper part of thermoelectric-bonded materials as follows.

$$[N(t_{10}) + iT(t_{10})]_1 = [N(t_{10}) + iT(t_{10})]_{11} + [N(t_{10}) + iT(t_{10})]_{12} \quad (43)$$

$$[N(t_{20}) + iT(t_{20})]_2 = [N(t_{20}) + iT(t_{20})]_{22} + [N(t_{20}) + iT(t_{20})]_{21}. \quad (44)$$

First, we need to find the equation of the first crack L_1 that lies in the upper part of thermoelectric-bonded materials as shown in Figure 4.

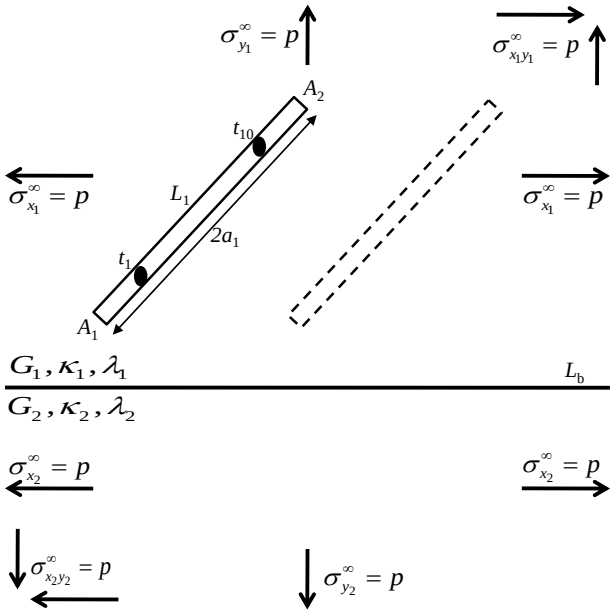

Figure 4. First crack L_1 in the upper part of thermoelectric-bonded materials subjected to remote stress.

By applying Equation (38), the first crack L_1 is obtained when the observation point is placed at the point $z = t_{10}$ and $dz = dt_{10}$, caused by COD function $(g_1(t_1))$ along the crack L_1 gives:

$$[N(t_{10}) + iT(t_{10})]_{11} = \frac{1}{\pi} \oint_{L_1} \frac{g_1(t_1)dt_1}{(t_1 - t_{10})^2} + \frac{1}{2\pi} \int_{L_1} M_1(t_1, t_{10}) g_1(t_1) dt_1 + \frac{1}{2\pi} \int_{L_1} M_2(t_1, t_{10}) \overline{g_1(t_1)} dt_1 + M_3(a_1, t_{10}). \quad (45)$$

Second, we need to find the equation of the second crack L_2 that lies in the upper part of thermoelectric-bonded materials, as shown in Figure 5.

Then, the second crack L_2 is obtained when the observation point is placed at the point $z = t_{10}$ and $dz = dt_{10}$, caused by COD function $(g_2(t_2))$ along the crack L_2 gives:

$$[N(t_{20}) + iT(t_{20})]_{22} = \frac{1}{\pi} \oint_{L_2} \frac{g_2(t_2)dt_2}{(t_2 - t_{20})^2} + \frac{1}{2\pi} \int_{L_2} M_1(t_2, t_{20}) g_2(t_2) dt_2 + \frac{1}{2\pi} \int_{L_2} M_2(t_2, t_{20}) \overline{g_2(t_2)} dt_2 + M_3(a_2, t_{20}). \quad (46)$$

By considering both cracks that lie in the upper part of thermoelectric-bonded materials as shown in Figure 4, the equation of the crack L_1 that is influenced by the COD function $(g_2(t_2))$ along the crack L_2 gives:

$$[N(t_{10}) + iT(t_{10})]_{12} = \frac{1}{\pi} \int_{L_2} \frac{g_2(t_2)dt_2}{(t_2 - t_{10})^2} + \frac{1}{2\pi} \int_{L_2} E_1(t_2, t_{10}) g_2(t_2) dt_2 + \frac{1}{2\pi} \int_{L_2} E_2(t_2, t_{10}) \overline{g_2(t_2)} dt_2 + M_3(a_2, t_{10}). \quad (47)$$

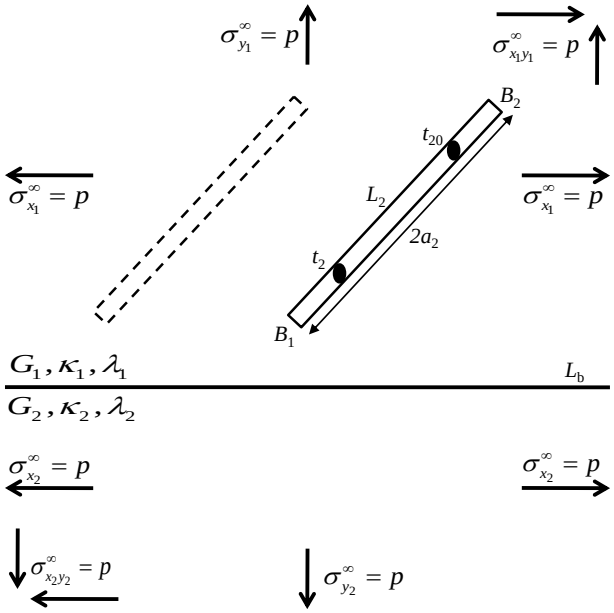

Figure 5. Second crack L_2 in the upper part of thermoelectric-bonded materials subjected to remote stress.

By using superposition principle of the COD function $g_1(t_1)$ along the crack L_1 (45) and COD function $g_2(t_2)$ along the crack L_2 (47), the HSIEs for crack L_1 are obtained as follows.

$$\begin{aligned}[N(t_{10}) + iT(t_{10})]_1 = {} & \frac{1}{\pi} \oint_{L_1} \frac{g_1(t_1)dt_1}{(t_1 - t_{10})^2} + \frac{1}{2\pi} \int_{L_1} M_1(t_1, t_{10}) g_1(t_1) dt_1 + \frac{1}{2\pi} \int_{L_1} M_2(t_1, t_{10}) \overline{g_1(t_1)} dt_1 \\ & + M_3(a_1, t_{10}) + \frac{1}{\pi} \int_{L_2} \frac{g_2(t_2)dt_2}{(t_2 - t_{10})^2} + \frac{1}{2\pi} \int_{L_2} M_1(t_2, t_{10}) g_2(t_2) dt_2 \\ & + \frac{1}{2\pi} \int_{L_2} M_2(t_2, t_{10}) \overline{g_2(t_2)} dt_2 + M_3(a_2, t_{10}). \end{aligned} \tag{48}$$

Then, similar to the HSIEs for the crack L_2 is obtained as follows.

$$\begin{aligned}[N(t_{20}) + iT(t_{20})]_2 = {} & \frac{1}{\pi} \oint_{L_2} \frac{g_2(t_2)dt_2}{(t_2 - t_{20})^2} + \frac{1}{2\pi} \int_{L_2} M_1(t_2, t_{20}) g_2(t_2) dt_2 + \frac{1}{2\pi} \int_{L_2} M_2(t_2, t_{20}) \overline{g_2(t_2)} dt_2 \\ & + M_3(a_2, t_{20}) + \frac{1}{\pi} \int_{L_1} \frac{g_1(t_1)dt_1}{(t_1 - t_{20})^2} + \frac{1}{2\pi} \int_{L_1} M_1(t_1, t_{20}) g_1(t_1) dt_1 \\ & + \frac{1}{2\pi} \int_{L_1} M_2(t_1, t_{20}) \overline{g_1(t_1)} dt_1 + M_3(a_1, t_{20}). \end{aligned} \tag{49}$$

Note that the first integral with the equal sign in Equations (48) and (49) represents the hypersingular integral and must be defined as a finite part integral.

4. Solutions for Crack Problems in Thermoelectric-Bonded Materials

4.1. Quadrature Formulas

In order to solve the HSIEs, the curved length coordinate method is used and defined as follows.

$$H(s) = \frac{g(t)}{\sqrt{a^2 - s^2}}. \tag{50}$$

Therefore, the HSIEs (38) for a crack in the upper part of thermoelectric-bonded materials give:

$$[N(t_0)+iT(t_0)]_1 = \frac{1}{\pi}\oint_L \frac{\sqrt{a^2-s^2}H(s)dt}{(t-t_0)^2} + \frac{1}{2\pi}\int_L M_1(t,t_0)\sqrt{a^2-s^2}H(s)dt + \frac{1}{2\pi}\int_L M_2(t,t_0)\sqrt{a^2-s^2}\overline{H(s)}dt + M_3(a,t_0) \tag{51}$$

By applying the following quadrature formulas, [44–47]

$$\frac{1}{\pi}\oint_{-a}^{a} \frac{\sqrt{a^2-s^2}H(s)ds}{(s-s_0)^2} \simeq \sum_{j=1}^{M+1} W_j(s_0)H(s_j), \tag{52}$$

$$\frac{1}{\pi}\int_{-a}^{a} \sqrt{a^2-s^2}H(s)ds \simeq \frac{1}{M+2}\sum_{j=1}^{M+1}(a^2-s_0^2)H(s_j), \tag{53}$$

Equation (51) then yields:

$$[N(t_0)+iT(t_0)]_1 = \sum_{j=1}^{M+1} W_j(s_0)H(s_j)\frac{(s-s_0)^2}{(t-t_0)^2}\frac{dt}{ds} + \frac{1}{2M+4}\sum_{j=1}^{M+1}(a^2-s_0^2)H(s_j)M_1(t,t_0)\frac{dt}{ds} + \frac{1}{2M+4}\sum_{j=1}^{M+1}(a^2-s_0^2)\overline{H(s_j)}M_2(t,t_0)\frac{dt}{ds} + M_3(a,t_0) \tag{54}$$

where $H(s_j)$ is a given function, $M \in \mathbb{Z}^+$ is subdivision numbers of the cracks,

$$s_j = a\cos\left(\frac{j\pi}{M+2}\right),\ j = 1,2,...,M+1,$$

and

$$W_j(s_0) = -\frac{2}{M+2}\sum_{n=0}^{M}(n+1)\sin\left(\frac{j\pi}{M+2}\right)\sin\left(\frac{(n+1)j\pi}{M+2}\right)U_n\left(\frac{s_{j0}}{a}\right),$$

and the observation points

$$s_0 = s_{0,k} = a\cos\left(\frac{k\pi}{M+2}\right),\ k = 1,2,...,M+1.$$

Here, $U_n(t)$ is a Chebyshev polynomial of the second kind, defined by

$$U_n(t) = \frac{\sin((n+1)\theta)}{\sin\theta}, \text{where } t = \cos\theta. \tag{55}$$

Similar to the HSIEs (48) and (49) two cracks in the upper part of thermoelectric-bonded materials give:

$$\begin{aligned}[N(t_{10})+iT(t_{10})]_1 = {} & \sum_{j=1}^{M+1} W_j(s_{10})H_1(s_j)\frac{(s_1-s_{10})^2}{(t_1-t_{10})^2}\frac{dt_1}{ds_1} + \frac{1}{2M+4}\sum_{j=1}^{M+1}(a_1^2-s_{10}^2)H_1(s_j)M_1(t_1,t_{10})\frac{dt_1}{ds_1} \\ & + \frac{1}{2M+4}\sum_{j=1}^{M+1}(a_1^2-s_{10}^2)\overline{H_1(s_j)}M_2(t_1,t_{10})\frac{dt_1}{ds_1} + M_3(a_1,t_{10}) \\ & + \frac{1}{M+2}\sum_{j=1}^{M+1}(a_2^2-s_{10}^2)H_2(s_j)\frac{1}{(t_2-t_{10})^2}\frac{dt_2}{ds_2} + \frac{1}{2M+4}\sum_{j=1}^{M+1}(a_2^2-s_{10}^2)H_2(s_j)M_1(t_2,t_{10})\frac{dt_2}{ds_2} \\ & + \frac{1}{2M+4}\sum_{j=1}^{M+1}(a_2^2-s_{10}^2)\overline{H_2(s_j)}M_2(t_2,t_{10})\frac{dt_2}{ds_2} + M_3(a_2,t_{10}).\end{aligned} \tag{56}$$

$$[N(t_{20})+iT(t_{20})]_2=\sum_{j=1}^{M+1}W_j(s_{20})H_2(s_j)\frac{(s_2-s_{20})^2}{(t_2-t_{20})^2}\frac{dt_2}{ds_2}+\frac{1}{2M+4}\sum_{j=1}^{M+1}(a_2^2-s_{20}^2)H_2(s_j)M_1(t_2,t_{20})\frac{dt_2}{ds_2}$$
$$+\frac{1}{2M+4}\sum_{j=1}^{M+1}(a_2^2-s_{20}^2)\overline{H_2(s_j)}M_2(t_2,t_{20})\frac{dt_2}{ds_2}+M_3(a_2,t_{20})$$
$$+\frac{1}{M+2}\sum_{j=1}^{M+1}(a_1^2-s_{20}^2)H_1(s_j)\frac{1}{(t_1-t_{20})^2}\frac{dt_1}{ds_1}+\frac{1}{2M+4}\sum_{j=1}^{M+1}(a_1^2-s_{20}^2)H_1(s_j)M_1(t_1,t_{20})\frac{dt_1}{ds_1}$$
$$+\frac{1}{2M+4}\sum_{j=1}^{M+1}(a_1^2-s_{20}^2)\overline{H_1(s_j)}M_2(t_1,t_{20})\frac{dt_1}{ds_1}+M_3(a_1,t_{20}). \tag{57}$$

4.2. Stress Intensity Factors

In order to investigate the behavior of non-dimensional SIFs for crack problems in thermoelectric-bonded materials subjected to remote stress, we define the SIFs at the crack tips A_j and B_j as follows:

$$K_{A_j}=(K_1-iK_2)_{A_j}=\sqrt{2\pi}\lim_{t\to t_{A_j}}\sqrt{|t-t_{A_j}|}g_1'(t_1),\qquad j=1,2, \tag{58}$$

$$K_{B_j}=(K_1-iK_2)_{B_j}=\sqrt{2\pi}\lim_{t\to t_{B_j}}\sqrt{|t-t_{B_j}|}g_2'(t_2),\qquad j=1,2, \tag{59}$$

where $g_1'(t_1)$ and $g_2'(t_2)$ are defined as follows:

$$g_k'(t_k)|_{t_k=t_k(s_k)}=\frac{-s_kH_k(s_k)}{\sqrt{a_k^2-s_k^2}}e^{-i\theta_{A_j}},\qquad H_k'(s_k)=0, \tag{60}$$

and $k=1,2$. Therefore, the non-dimensional SIFs at crack tips A_j and B_j are defined as follows.

$$K_{A_j}=(K_1-iK_2)_{A_j}=\sqrt{2\pi}\lim_{s\to s_{A_j}}\sqrt{|s-s_{A_j}|}\left[\frac{-s_1H_1(s_1)}{\sqrt{a_1^2-s_1^2}}e^{-i\theta_{A_j}}\right]=\sqrt{a_1\pi}F_{A_j}, \tag{61}$$

$$K_{B_j}=(K_1-iK_2)_{B_j}=\sqrt{2\pi}\lim_{s\to s_{B_j}}\sqrt{|s-s_{B_j}|}\left[\frac{-s_2H_2(s_2)}{\sqrt{a_2^2-s_2^2}}e^{-i\theta_{B_j}}\right]=\sqrt{a_2\pi}F_{B_j}, \tag{62}$$

where

$$F_{A_j}=H_1(-a_1)e^{-i\theta_{A_j}}=F_{1A_j}+iF_{2A_j},$$
$$F_{B_j}=H_2(-a_2)e^{-i\theta_{B_j}}=F_{1B_j}+iF_{2B_j}.$$

At crack tips A_j and B_j, F_{1A_j} and F_{1B_j} represent the Mode I non-dimensional SIFs, which characterize the intensity of the normal stress singularity. In contrast, F_{2A_j} and F_{2B_j} represent the Mode II non-dimensional SIFs at the same crack tips, describing the magnitude of the shear stress singularity.

Table 1 displays convergence test results on the Mode I (F_1) dimensionless SIFs versus h/a at the crack tips A_1 and A_2 for an inclined crack in the upper part of thermoelectric-bonded materials for $\alpha=90^\circ$, $\mathbf{J}=20$, and $\mathbf{U}=0$ as illustrated in Figure 2 using material parameters in Table 2.

Table 1. Convergence test result on dimensionless SIFs at the crack tips A_1 and A_2 for an inclined crack as illustrated in Figure 2.

G_2/G_1	M	SIFs	h/a				
			1.2	**1.4**	**1.6**	**1.8**	**2.0**
0.25	10	F_{1A_1}	1.2241	1.1302	1.0888	1.0659	1.0517
		F_{1A_2}	1.0835	1.0622	1.0498	1.0418	1.0365
	15	F_{1A_1}	1.2254	1.1316	1.0904	1.0677	1.0538
		F_{1A_2}	1.0862	1.0651	1.0531	1.0456	1.0408
	20	F_{1A_1}	1.2267	1.1330	1.0920	1.0695	1.0559
		F_{1A_2}	1.0888	1.0680	1.0564	1.0493	1.0451
	22	F_{1A_1}	1.2267	1.1330	1.0920	1.0695	1.0559
		F_{1A_2}	1.0888	1.0680	1.0564	1.0493	1.0451
2.00	10	F_{1A_1}	0.9102	0.9499	0.9704	0.9835	0.9933
		F_{1A_2}	0.9844	0.9966	1.0063	1.0148	1.0226
	15	F_{1A_1}	0.9139	0.9545	0.9761	0.9906	1.0019
		F_{1A_2}	0.9939	1.0082	1.0201	1.0310	1.0415
	20	F_{1A_1}	0.9175	0.9592	0.9819	0.9978	1.0108
		F_{1A_2}	1.0036	1.0199	1.0342	1.0476	1.0609
	22	F_{1A_1}	0.9175	0.9592	0.9819	0.9978	1.0108
		F_{1A_2}	1.0036	1.0199	1.0342	1.0476	1.0609

Table 2. Parameters for the thermoelectric-bonded materials.

$\lambda_1 = \lambda_2$	$\kappa_1 = \kappa_2$	$E_1 = E_2$	$\alpha_1 = \alpha_2$	$\mu_1 = \mu_2$
4×10^4	10	196	5.2×10^{-6}	0.283

The accuracy of the numerical results relies on the level of subdivision for the cracks, denoted as M. To assess result convergence, we systematically increase the value of M, starting from $M = 10$ and progressing to $M = 15, 20$. Eventually, we halt at $M = 22$ as the dimensionless SIFs values align with the previous M as presented in Table 1. Notably, it is observed that smaller values of M yield convergent numerical results. In addition to the HSIEs approach discussed in this study, the dimensionless SIFs with $\mathbf{J} = \mathbf{U} = 0$ are validated using the body force method approach introduced by Isida and Noguchi [48]. These results, along with the SIFs from the HSIEs approach, are listed in Table 3. It is noteworthy that the disparity between the results obtained from these two approaches is minimal. It is found that the maximum percentage error (%ϵ) is 0.0809% which is a very minimal percentage of error between the results of the current study and previous study.

Table 3. Validation test result and percentage error (%ϵ) on dimensionless SIFs at the crack tips A_1 and A_2 compared with Isida and Noguchi [48].

G_2/G_1	M	SIFs and %ϵ	h/a				
			1.2	**1.4**	**1.6**	**1.8**	**2.0**
0.25	20	F_{1A_1} *	1.2213	1.1274	1.0857	1.0623	1.0476
		F_{1A_1} **	1.2220	1.1280	1.0860	1.0630	1.0480
		%ϵ F_{1A_1}	0.0573	0.0532	0.0276	0.0659	0.0362
		F_{1A_2} *	1.0783	1.0563	1.0432	1.0344	1.0281
		F_{1A_2} **	1.0790	1.0570	1.0430	1.0350	1.0280
		%ϵ F_{1A_2}	0.0649	0.0662	0.0192	0.0580	0.0097

Table 3. *Cont.*

G_2/G_1	M	SIFs and %ϵ	*h*/*a*				
			1.2	**1.4**	**1.6**	**1.8**	**2.0**
0.50	20	F_{1A_1} *	1.1111	1.0653	1.0444	1.0324	1.0249
		F_{1A_1} **	1.1120	1.0660	1.0450	1.0330	1.0250
		%ϵ F_{1A_1}	0.0809	0.0657	0.0574	0.0581	0.0097
		F_{1A_2} *	1.0394	1.0289	1.0223	1.0179	1.0147
		F_{1A_2} **	1.0400	1.0290	1.0220	1.0180	1.0150
		%ϵ F_{1A_2}	0.0577	0.0097	0.0294	0.0097	0.0296
2.00	20	F_{1A_1} *	0.9032	0.9410	0.9592	0.9699	0.9767
		F_{1A_1} **	0.9030	0.9410	0.9590	0.9700	0.9770
		%ϵ F_{1A_1}	0.0221	0.0000	0.0209	0.0103	0.0307
		F_{1A_2} *	0.9656	0.9740	0.9795	0.9834	0.9863
		F_{1A_2} **	0.9660	0.9740	0.9790	0.9830	0.9860
		%ϵ F_{1A_2}	0.0414	0.0000	0.0511	0.0407	0.0304
4.00	20	F_{1A_1} *	0.8291	0.8944	0.9266	0.9455	0.9579
		F_{1A_1} **	0.8290	0.8940	0.9270	0.9450	0.9580
		%ϵ F_{1A_1}	0.0121	0.0447	0.0431	0.0529	0.0104
		F_{1A_2} *	0.9393	0.9535	0.9631	0.9701	0.9752
		F_{1A_2} **	0.9390	0.9540	0.9630	0.9700	0.9750
		%ϵ F_{1A_2}	0.0319	0.0524	0.0104	0.0103	0.0205

* Current study, ** Isida and Noguchi [48].

5. Concluding Remarks

In this study, we have dealt with crack problems in the upper part of thermoelectric-bonded materials subjected to remote stress. Although the problem is an ancient one, we insist on several novelties in this study. First, even though the modified complex potential method used in this work is a traditional technique for solving crack problems in bonded materials, it is, however, new for cases that involve crack problems in thermoelectric materials. The present approach leads to HSIEs in which the COD function, electric current density, and energy flux load between the crack tips are taken as the main unknown. The general solution of HSIEs for the single- and two-crack problems have been obtained. The validation of the HSIEs has been proved by reducing them to infinite materials where $G_1 = G_2$, $K_1 = K_2$, and $E_1 = E_2$, and the values of $\alpha_1 = \alpha_2 = 0$ and $\lambda_1 = \lambda_2 = 0$. Meanwhile, HSIEs reduce to half-plane materials if $G_2 = 0$, and the values of $\alpha_1 = \alpha_2 = 0$, $\lambda_1 = \lambda_2 = 0$ and $\kappa_2 = 0$. In the context of the test problems, our numerical findings demonstrate faster convergence, and the results obtained from our analysis align with those from the previous study with a very minimal percentage of error. On the basis of this study, we believe that several extensions are possible, such as cohesive models, cracks at the interface-bonded materials, cracks issued by inclusions, problems of three-dimensional cracks in thermoelectric-bonded materials, and so on. Based on the current study, a detailed formulation with numerical analysis will be published elsewhere. More research is being conducted to broaden the application field of the developed concept.

Author Contributions: Conceptualization, M.H.I.M.N., K.B.H., N.S.K. and N.M.A.N.L.; methodology, M.H.I.M.N., K.B.H. and I.W.; software, M.H.I.M.N. and K.B.H.; validation, K.B.H., N.M.A.N.L. and S.F.; formal analysis, M.H.I.M.N., K.B.H. and N.M.A.N.L.; writing—original draft preparation, M.H.I.M.N. and K.B.H.; writing—review and editing, K.B.H., N.S.K. and N.M.A.N.L.; supervision, K.B.H., I.W., N.M.A.N.L. and S.F. All authors have read and agreed to the published version of the manuscript.

Funding: This work is fully supported by the Ministry of Higher Education Malaysia through the Fundamental Research Grant Scheme (FRGS/1/2021/STG06/UTEM/03/2). The authors would like to thank the editor and anonymous reviewers for their valuable comments and suggestions that helped to improve this paper, and the Universiti Teknikal Malaysia Melaka (UTeM) for their support.

Data Availability Statement: Not applicable.

Conflicts of Interest: The authors declare no conflict of interest.

Abbreviations

The following abbreviations are used in this manuscript:

COD	Crack Opening Displacement
HSIEs	Hypersingular Integral Equations
SIFs	Stress Intensity Factors
$\phi(z)$, $\psi(z)$, $f(z)$, $g(z)$	Complex stress potential functions
$\phi_1(z)$, $\psi_1(z)$, $f_1(z)$, $g_1(z)$	Upper part of complex potential functions
$\phi_{1p}(z)$, $\psi_{1p}(z)$, $f_{1p}(z)$, $g_{1p}(z)$	Principal part of complex potential functions
$\phi_{1c}(z)$, $\psi_{1c}(z)$, $f_{1c}(z)$, $g_{1c}(z)$	Complementary part of complex potential functions
$\phi_2(z)$, $\psi_2(z)$, $f_2(z)$, $g_2(z)$	Lower part of complex potential functions
σ_x, σ_y, σ_{xy}	Stress components
G	Shear modulus
μ	Poisson's ratio
E	Young's modulus
$g(t)$	Crack opening displacement function
Γ_i	Elastic constant
K_{A_j}	Stress Intensity Factors at crack tip A_j
F_{A_j}	Dimensionless Stress Intensity Factors at crack tip A_j

References

1. Nik Long, N.M.A.; Eshkuvatov, Z.K. Hypersingular integral equation for multiple curved cracks problem in plane elasticity. *Int. J. Solids Struct.* **2009**, *46*, 2611–2617. [CrossRef]
2. Liu, Z.X.; Xu, W.; Yu, Y.; Wu, X.R. Weight Functions and Stress Intensity Factors for Two Unequal-Length Collinear Cracks in an Infinite Sheet. *Eng. Fract. Mech.* **2019**, *209*, 173–186. [CrossRef]
3. Ghajar, R.; Hajimohamadi, M. Analytical calculation of stress intensity factors for cracks emanating from a quasi-square hole in an infinite plane. *Theor. Appl. Fract. Mech.* **2019**, *99*, 71–78. [CrossRef]
4. Ghorbanpoor, R.; Nik Long, N.M.A.; Eshkuvatov, Z.K. Formulation for multiple curved crack problem in a finite plate. *Malays. J. Math. Sci.* **2016**, *10*, 253–263.
5. Zhang, J.; Qu, Z.; Liu, W.; Wang, L. Automated numerical simulation of the propagation of multiple cracks in a finite plane using the distributed dislocation method. *Comptes Rendus Mec.* **2019**, *347*, 191–206. [CrossRef]
6. Chen, Y.Z.; Lin, X.Y.; Wang, X.Z. Numerical solution for curved crack problem in elastic half-plane using hypersingular integral equation. *Philos. Mag.* **2009**, *89*, 2239–2253. [CrossRef]
7. Elfakhakhre, N.R.F.; Nik Long, N.M.A.; Eshkuvatov, Z.K. Stress intensity factor for an elastic half plane weakened by multiple curved cracks. *Appl. Math. Model.* **2018**, *60*, 540–551. [CrossRef]
8. Kebli, B.; Baka, Z. Annular crack in an elastic half-space. *Int. J. Eng. Sci.* **2019**, *134*, 117–147. [CrossRef]
9. Hamzah, K.B.; Nik Long, N.M.A.; Senu, N.; Eshkuvatov, Z.K.; Ilias, M.R. Stress intensity factors for a crack in bonded dissimilar materials subjected to various stresses. *Univers. J. Mech. Eng.* **2019**, *7*, 179–189. [CrossRef]
10. Chai, H.; Lv, J.; Bao, Y. Numerical solutions of hypersingular integral equations for stress intensity factors of planar embedded interface cracks and their correlations with bimaterial parameters. *Int. J. Solids Struct.* **2020**, *202*, 184–194. [CrossRef]
11. Hamzah, K.B.; Nik Long, N.M.A.; Senu, N.; Eshkuvatov, Z.K. Stress intensity factor for bonded dissimilar materials weakened by multiple cracks. *Appl. Math. Model.* **2020**, *77*, 585–601. [CrossRef]
12. Long, G.; Liu, Y.; Xu, W.; Zhou, P.; Zhou, J.; Xu, G.; Xiao, B. Analysis of crack problems in multilayered elastic medium by a consecutive stiffness method. *Mathematics* **2022**, *10*, 4403. [CrossRef]
13. Salha, L.; Bleyer, J.; Sab, K.; Bodgi, J. A hybridized mixed approach for efficient stress prediction in a layerwise plate model. *Mathematics* **2022**, *10*, 1711. [CrossRef]
14. Elfakhakhre, N.R.F.; Nik Long, N.M.A.; Eshkuvatov, Z.K. Numerical solutions for cracks in an elastic half-plane. *Acta Mech. Sin.* **2019**, *35*, 212–227. [CrossRef]
15. Hamzah, K.B.; Nik Long, N.M.A.; Senu, N.; Eshkuvatov, Z.K. Numerical solution for crack phenomenon in dissimilar materials under various mechanical loadings. *Symmetry* **2021**, *13*, 235. [CrossRef]

16. Aguirre-Mesa, A.M.; Restrepo-Velasquez, S.; Ramirez-Tamayo, D.; Montoya, A.; Millwater, H. Computation of two dimensional mixed-mode stress intensity factor rates using a complex-variable interaction integral. *Eng. Fract. Mech.* **2023**, *277*, 108981. [CrossRef]
17. Zhang, X.Y.; Xie, Y.J.; Li, X.F. Transient thermoelastic response in a cracked strip of functionally graded materials via generalized fractional heat conduction. *Appl. Math. Model.* **2019**, *70*, 328–349. [CrossRef]
18. Hamzah, K.B.; Nik Long, N.M.A.; Senu, N.; Eshkuvatov, Z.K. Numerical solution for the thermally insulated cracks in bonded dissimilar materials using hypersingular integral equations. *Appl. Math. Model.* **2021**, *91*, 358–373. [CrossRef]
19. Hobiny, A.; Abbas, I.A. A study on the thermoelastic interaction in two-dimension orthotropic materials under the fractional derivative model. *Alex. Eng. J.* **2023**, *64*, 615–625. [CrossRef]
20. Lin, C.B.; Chen, S.C.; Lee, J.L. Explicit solutions of magnetoelastic fields in a soft ferromagnetic solid with curvilinear cracks. *Eng. Fract. Mech.* **2009**, *76*, 1846–1865. [CrossRef]
21. Xiao, J.; Feng, G.; Su, M.; Xu, Y.; Zhang, F. Fracture analysis on periodic radial cracks emanating from a nano-hole with surface effects in magnetoelectroelastic materials. *Eng. Fract. Mech.* **2021**, *258*, 108115. [CrossRef]
22. Mouley, J.; Sarkar, N.; De, S. Griffith crack analysis in nonlocal magneto-elastic strip using Daubechies wavelets. *Waves Random Complex Media* **2023**, 1–19. [CrossRef]
23. Wang, P.; Wang, B.L.; Wang, K.F. Dynamic response of cracked thermoelectric materials. *Int. J. Mech. Sci.* **2019**, *160*, 298–306. [CrossRef]
24. Jiang, D.; Luo, Q.H.; Liu, W.; Zhou, Y.T. Thermoelectric field disturbed by two unequal cracks adjacent to a hole in thermoelectric materials. *Eng. Fract. Mech.* **2020**, *235*, 107163. [CrossRef]
25. Zheng, M.; Gao, C.F. An arc-shaped crack in an electrostrictive material. *Int. J. Eng. Sci.* **2010**, *48*, 771–782. [CrossRef]
26. Zhang, A.B.; Wang, B.L. Crack tip field in thermoelectric media. *Theor. Appl. Fract. Mech.* **2013**, *66*, 33–36. [CrossRef]
27. Song, H.P.; Gao, C.F.; Li, J. Two-dimensional problem of a crack in thermoelectric materials. *J. Therm. Stress.* **2015**, *38*, 325–337. [CrossRef]
28. Zhang, A.B.; Wang, B.L. Explicit solutions of an elliptic hole or a crack problem in thermoelectric materials. *Eng. Fract. Mech.* **2016**, *151*, 11–21. [CrossRef]
29. Yu, C.; Zou, D.; Li, Y.H.; Yang, H.B.; Gao, C.F. An arc-shaped crack in nonlinear fully coupled thermoelectric materials. *Acta Mech.* **2018**, *229*, 1989–2008. [CrossRef]
30. Zhang, A.B.; Wang, B.L.; Wang, J.; Du, J.K. Two-dimensional problem of thermoelectric materials with an elliptic hole or a rigid inclusion. *Int. J. Therm. Sci.* **2017**, *117*, 184–195. [CrossRef]
31. Yu, C.B.; Yang, H.B.; Li, Y.H.; Song, K.; Gao, C.F. Closed-form solutions for a circular inhomogeneity in nonlinearly coupled thermoelectric materials. *Zamm-J. Appl. Math. Mech. Angew. Math. Mech.* **2019**, *99*, e201800240. [CrossRef]
32. Liu, Y.; Wang, B.L.; Li, J.E.; Wang, K.F. Thermoelectric and stress fields for a cracked thermoelectric media based on the electric field saturation model. *Mech. Res. Commun.* **2020**, *104*, 103479. [CrossRef]
33. Song, K.; Song, H.P.; Schiavone, P.; Gao, C.F. Electric current induced thermal stress around a bi-material interface crack. *Eng. Fract. Mech.* **2019**, *208*, 1–12. [CrossRef]
34. Sladek, J.; Sladek, V.; Repka, M.; Schmauder, S. Crack analysis of nano-sized thermoelectric material structures. *Eng. Fract. Mech.* **2020**, *234*, 107078. [CrossRef]
35. Cui, Y.J.; Wang, B.L.; Wang, K.F.; Wang, G.G.; Zhang, A.B. An analytical model to evaluate the fatigue crack effects on the hybrid photovoltaic-thermoelectric device. *Renew. Energy* **2022**, *182*, 923–933. [CrossRef]
36. Jiang, D.; Zhou, Y.T. Role of crack length, crack spacing and layer thickness ratio in the electric potential and temperature of thermoelectric bi-materials systems. *Eng. Fract. Mech.* **2022**, *259*, 108170. [CrossRef]
37. Chan, Y.S.; Fannjiang, A.C.; Paulino, G.H. Integral equations with hypersingular kernels—Theory and applications to fracture mechanics. *Int. J. Eng. Sci.* **2003**, *41*, 683–720. [CrossRef]
38. Dutta, B.; Banerjea, S. Solution of a hypersingular integral equation in two disjoint intervals. *Appl. Math. Lett.* **2009**, *22*, 1281–1285. [CrossRef]
39. Ghorbanpoor, R.; Jafar, S.N.; Nik Long, N.M.A.; Majid, E. Stress intensity factor for multiple cracks in an infinite plate using hypersingular integral equations. *Comput. Methods Differ. Equ.* **2020**, *8*, 69–84.
40. Elahi, M.R.; Mahmoudi, Y.; Salimi Shamloo, A.; Jahangiri Rad, M. A novel collocation method for numerical solution of hypersingular integral equation with singular right-hand function. *Adv. Math. Physics* **2023**, *2023*, 5845263. [CrossRef]
41. Bergman, D.J.; Levy, O. Thermoelectric properties of a composite medium. *J. Appl. Phys.* **1991**, *70*, 6821–6833. [CrossRef]
42. Chen, Y.Z.; Hasebe, N. Stress-intensity factors for curved circular crack in bonded dissimilar materials. *Theor. Appl. Fract. Mech.* **1992**, *17*, 189–196. [CrossRef]
43. Hamzah, K.B.; Nik Long, N.M.A.; Senu, N.; Eshkuvatov, Z.K. Stress intensity factor for multiple cracks in bonded dissimilar materials using hypersingular integral equations. *Appl. Math. Model.* **2019**, *73*, 95–108. [CrossRef]
44. Mayrhofer, K.; Fischer, F.D. Derivation of a new analytical solution for a general two-dimensional finite-part integral applicable in fracture mechanics. *Int. J. Numer. Method Eng.* **1992**, *33*, 1027–1047. [CrossRef]
45. Mason, T.C.; Handscomb, D.C. *Chebyshev Polynomials*; Chapman and Hall/CRC: Boca Raton, FL, USA, 2003.
46. Kythe, P.K.; Schaferkotter, M.R. *Handbook of Computational Methods for Integration*; Chapman and Hall/CRC: Boca Raton, FL, USA, 2004.

47. Monegato, G. Numerical evaluation of hypersingular integrals. *J. Comput. Appl. Math.* **1994**, *50*, 9–31. [CrossRef]
48. Isida, M.; Noguchi, H. Arbitrary array of cracks in bonded half planes subjected to various loadings. *Eng. Fract. Mech.* **1993**, *46*, 365–380. [CrossRef]